Pure appl. geophys. 152 (1998) 707–731
0033–4553/98/040707–25 $ 1.50 + 0.20/0

Pure and Applied Geophysics

Instrumental Seismicity of the Western Alps: A Revised Catalogue

MARC NICOLAS,[1] NICOLE BETHOUX[2] and BRIGITTE MADEDDU[2]

Abstract—The western Alpine regions have been instrumented since the beginning of the century, and the number of seismological stations largely increased since 1980. This dense network has allowed an important improvement in the hypocentral determination, even for low magnitude events. This condition was a good opportunity to perform a synthesis of 32 years of instrumental seismicity in the Western Alps and southeast of France (1962–1993) and to attempt an improvement of the older event location with the assistance of the more recent locations.

The revised catalogue of seismicity is built using station corrections and regional crustal models. After the elimination of non-natural events, the catalogue is composed of 6697 events. Another improvement corresponds to the revision of magnitudes. We performed several tests to evaluate the reliability of our results: location of quarry events and rock bursts, epicentral correlation with geological features, coherence in depth with interpreted seismic profile (ECORS line), Moho isobaths. A first use of this catalogue is presented for the Haute-Ubaye region in the southwestern Alps.

Key words: Seismicity, Alps, France, fault-plane solutions.

Introduction

Although the Western Alps (Fig. 1) are known to have a moderate seismicity, some large earthquakes have occurred. For example, the Basel earthquake in 1356 was felt over an area of 800 000 km^2 and, according to historical chronicles, reached a maximum intensity IX (MSK) (LEVRET *et al.*, 1994).

The return period of the large shocks ($I_0 \geq$ VIII) evaluated by some authors using very different methods is very long. HENDRICKX (1981) deduced periods in the range of 100 up to 450 years, according to the region, from a statistical analysis of the historical seismicity. BECK *et al.* (1996) studied sedimentary records in the Annecy Lake and evaluated the recurrence time intervals between late Quaternary seismic events to be between 200 and 550 years. Paleoseismicity and historical seismicity are probably most appropriate to characterize such a tectonic region with

[1] C.E.A. Laboratoire de Détection et de Géophysique, BP 12, 91680 Bruyères-le-Chatel, France.
[2] UMR Géosciences-Azur, CNRS, rue A. Einstein, Sophia-Antipolis, 06560 Valbonne, France.

long-return periods of large events. The study of instrumental seismicity on the longest possible period can however provide useful information to better define the seismogenic areas where microseisms usually occur and to provide seismotectonic knowledge with the aid of focal mechanism determinations.

Our primary goal in this study was to build a catalogue of instrumental seismicity, including old events, as reliable and homogeneous as possible.

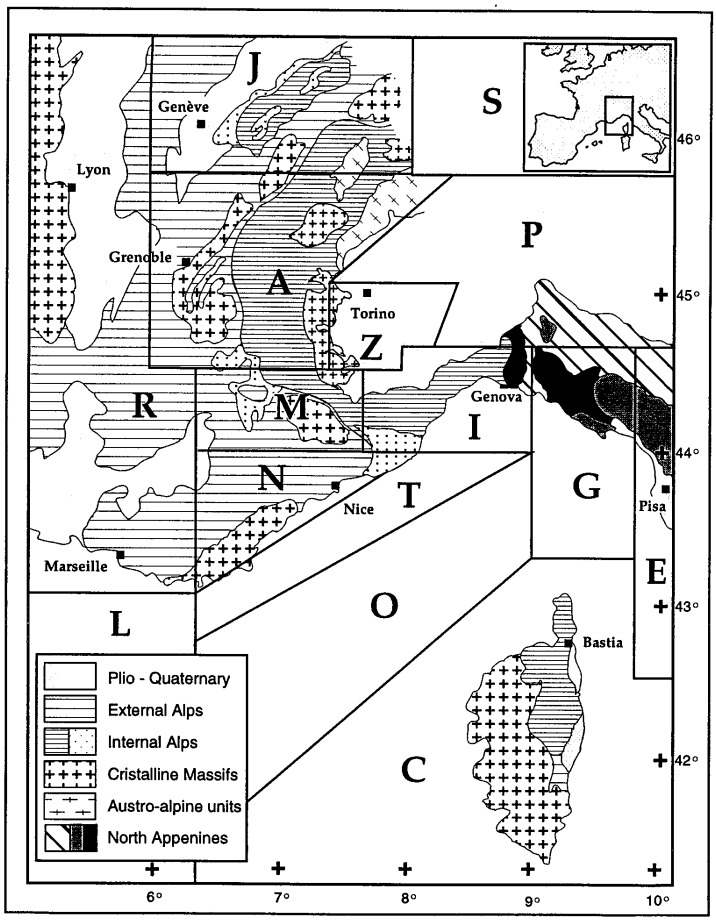

Figure 1
Simplified tectonic map of the Western Alpine chain, showing the area where each crustal model is applied. A: Alpine model, C: Corsican model, E: Appenine model, G: Genoa model, I: Italian model, J: Jura model, L: LDG model, M: Mercantour-Argentera model, N: Nice model, O: Oceanic model, P: Po plain model, R: Rhône valley model, S: Swiss model, T: Continental slope model, Z: Ivrea zone model.

The major difficulty in this exercise is that the number and locations of the seismological stations has changed considerably over recent decades. The Alpine regions have been early instrumented (Strasbourg as early as 1895, Trieste in 1911, Basel, Chur and Zürich in 1912, Firenze in 1924) and the number of the seismological stations has largely increased since 1980. There were about 35 stations around the Western Alps in 1955 and about 250 in 1990. In addition, the quality of records and data processing has significantly improved over that period.

Currently, some dense regional networks provide very accurate location thanks to numerous and high quality stations surrounding the seismic zones (ETH[1], DISTER[1], ReNaSS[1], SISMALP[1]). It was not our ambition to compete with these networks, on the contrary we wished to use the data and location obtained for the recent years in order to improve the location of the past events (located with less arrival times), or, at least, to estimate the errors on epicentral parameters more accurately.

Hereafter we explain how we built the revised catalogue (1962–1993) and tested the reliability of the revised locations. Then we performed location of some of the largest events between 1955 and 1961.

Finally we focus on a small region of the Western Alps (the Briançonnais-Ubaye region) and show that the revised seismicity highlights tectonic processes in this area.

The 1962–1993 Period

The Building of the Catalogue

In this section we describe the procedure that we have followed to build a complete and reliable catalogue for the area [41°N 5°E–47°N 10°E] and explain why the LDG/CEA[2] bulletin has been the basic framework of our revised bulletin. The first seismological stations of the LDG/CEA French network were installed in Northwestern France in 1957, in the north of Massif Central in 1960 and in the Southern Alps in 1962. The network was centralized and telemetered in 1974. We benefit from the entire corresponding seismograms which is necessary to revise the

[1] ETH: Institut fur Geophysik, Zürich, Switzerland; DISTER: Dipartimento di Scienze della Terra, Genova, Italy; SISMALP: Laboratoire de Geophysique Interne et Tectonophysique, Grenoble, France; ReNaSS: Réseau National de Surveillance Sismique, Strasbourg, France.

[2] LDG/CEA: Laboratoire de détection et de géophysique, Bruyères-le Châtel, France; ISC: International Seismological Centre, Newbury, United Kingdom; ING: Instituto Nazionale di Geofisica, Roma, Italy.

regional magnitude scale and to improve the magnitude of the older events. In addition, a preliminary study was performed from these data to discriminate natural and artificial events and to investigate the exact location of most of the artificial events (location of the main quarries, marine shot location obtained with cooperation of the Navy, rockbursts in the mines). In a first step these events are kept in the bulletin and identified with a special code.

From 1962 to 1988 the ISC[2] catalogue, which is a compilation of most of the data available, and LDG/CEA data were combined. For the most recent period we did not yet benefit from ISC compilation. We have formed the DISTER catalogue which already contained the ETH, ING[2], ReNaSS, and SISMALP data (KISSLING *et al.*, 1995) with the LDG/CEA data.

For both periods, data from isolated stations were also added. This was especially useful for the oldest events. The combination of data sources has been done algorithmically. This automatic data association was supervised in order to avoid erroneous associations of events with close origin times.

Classical location routines such as Hypo 71 (LEE and LAHR, 1975), Hypoinverse (KLEIN, 1978), and Hypoellipse (LAHR, 1980) take into account only one P-wave first arrival time and one S-wave arrival time. One test performed in these algorithms checks the best solution (direct or refracted raypath) for the corresponding P and S data according to the minimum discrepancy between the observed and theoretical travel time of these waves ($o-c$ arrival times). In order to optimize the use of available seismograms by duplicating the number of reading data and to improve on the focal depth determinations, the algorithm written at LDG/CEA considers both P_n and P_g phases (correlatively S_n and S_g phases). Consequently, P or S phases reported in some bulletins (Swiss or Italian) were to be differentiated into P_g or P_n, S_g or S_n. On the other hand, the P_b or P_mP phases reported in the long-established bulletins had to be identified as P_g, P_n or removed. Due to the geological complexity of the Alps, this choice was not trivial and this step was accomplished by hand event after event, after several location trials.

The standard location algorithm in use at LDG/CEA is based on the GEIGER method (1910). Origin time, epicentral longitude and latitude are deduced by inversion of the matrix of ($o-c$) arrival times after some iterations which improve step by step the trial epicenter location. The depth is used as a parameter in the travel-time computation and the final depth value (tested by step of one kilometer) is the one which provides the best statistical results: rms on the ($o-c$) arrival times and axes of the confidence ellipse for location.

First the events were located with this routine using one crustal model adapted to better fit the average Moho depth under the Alps (Table 1a). 10 000 events representing 178 000 arrival times belong to this first bulletin.

In a second step a more sophisticated algorithm was used, taking into account the complexity of the Alpine domain. The region studied is divided into thirteen areas displayed on Figure 1: each of them is characterized by a crustal model

Table 1a

Standard crustal model used for the first locations of the events

Model	Depth (km)	V_p (km/s)	V_s (km/s)
L	0	3.00	1.75
	0.9	6.03	3.56
	31	8.16	4.65

chosen on the basis of seismic data (deep seismic profiles GEOTRAVERSE (BLUNDELL *et al.*, 1992), ECORS-CROP experiment (ROURE *et al.*, 1990) but also the seismic profiles performed during the International Year of Geophysics in 1958 (CLOSS and LABROUSTE, 1963), because of the lack of recent data in the southwestern Alps), and propagation laws used by SISMALP and DISTER networks.

Table 1b displays these crustal models, applied for P_g and S_g phases. The time-terms involved in the computation of P_n and S_n phase propagation-time are characteristics of the domain of the prelocated events and of the station (following the method in use in Hypoellipse routine but introducing in the computation both direct and refracted data).

The most recent events (1987–1993) were located first, because for this period we benefit from a good azimuthal coverage due to the dense network and from a very good time marks (GPS or DCF receivers), and reading of arrival times

Table 1b

Examples of regional crustal models used in a second step of the location procedure

Model	Depth (km)	V_p (km/s)	V_s (km/s)	Model	Depth (km)	V_p (km/s)	V_s (km/s)
A	0	5.30	3.13	N	0	3.00	1.73
	3	5.95	3.52		1	6.00	3.46
	27	6.60	3.91		12	6.20	3.58
	35	8.20	4.85		26	8.20	4.74
P	0	3.30	1.90	Z	0	3.50	2.02
	8	5.00	2.89		1	4.50	2.60
	15	6.30	3.64		2	5.80	3.35
	25	7.00	4.04		6	6.20	3.58
	30	8.00	4.62		26	7.40	4.30
					35	8.05	4.65
O	0	1.5	0	G	0	4.80	2.77
	2	4.4	2.6		1	6.50	3.75
	8	5.8	3.4		20	7.90	4.57
	10	6.9	4.1				
	14	8.0	4.7				

(centralized interpretation and digital data). The algorithm used for the location of these recent events introduces a correction factor into the arrival times which depends both on the crustal model used, corresponding to the epicentral area, and on the structure under the station. These station corrections smooth the incidence of lateral variation of crustal models on the estimation of earthquake parameters. The events of the bulletin, limited to the period 1970–1993, were located using these station corrections and local crustal models. For the older events the recording networks were too different, as seen above, from the recent networks. It has not been possible to compute correction factors for the oldest stations because many of them are closed. Consequently the non-balance between the corrected and uncorrected stations creates a bias which deteriorates the location (PAVLIS and BOOKER, 1983).

Another difficulty met during the construction of the catalogue is to discriminate the natural events from the quarry blasts, the rockbursts and the marine shots. Artificial events represent 90% of the recorded seismic events in France. These are identified thanks to the characteristics of the signal and location. By eliminating these events and shifting outside of the geographic frame chosen (5°E, 10°E–41°N, 47°N), the catalogue was reduced from 10 000 to 6697 events, for the period 1962–1993 (Fig. 2). In this catalogue the rms are generally small, from 0.2 s, for the best located events, up to 2 s for some of the first earthquakes of our catalogue; and the axes of the confidence ellipses, for the corresponding events, range from 1 km to 100 km. An example of the comparison between the previous and new locations is given in Table 2.

The pattern of seismicity corresponding to this catalogue seems to delineate two arcs (Fig. 2). ROTHÉ (1942) already noted these features and called them the 'Piémontais and Briançonnais arcs'. The external crystalline massifs are almost aseismic whereas the seismicity is concentrated around these massifs. The characteristics of this seismicity and the tectonic implications have been detailed in regional studies as those of BOSSOLASCO *et al.* (1972), PAVONI (1977), FRÉCHET (1978), FRÉCHET and PAVONI (1979), CAPONI *et al.* (1980), CATTANEO *et al.* (1987), DEICHMANN (1987), HOANG-TRONG *et al.* (1987), EVA *et al.* (1990), PAVONI and ROTH (1990), THOUVENOT *et al.* (1991), GUYOTON (1991), AUGLIERA *et al.* (1995). We present here the characteristics of the seismicity at the scale of the entire Western Alps and southeast of France, for a period covering most of the instrumental period, with the aim to obtain homogeneous data base which includes long past events (since 1950) as well as recent seismicity.

Accuracy of Locations and Analysis of the Results

Even though the results are statistically correct in terms of low rms and small confidence ellipses, it is known that these parameters represent only an optimal fit between the data and the crustal model used. Consequently a major question is open: which are the criteria to qualify the accuracy of an earthquake location?

Table 2

Focal solutions for the Haute-Ubaye region. The previous and revised locations are compared

No.	Date	Times (h:min:s)	Lat. (N) (old)	Lon. (E) (old)	z (km) (old)	Lat. (N) (new)	Lon. (E) (new)	z (km) (new)	M	Meca. ref.	Pl. 1 (Az. Dip)	Pl. 2 (Az. Dip)	P axes (Az. Dip)	T axes (Az. Dip)
1	05 04 59	10:48:00	44.53	6.78	8	—	—	—	5.3	FR*	170 70W	066 56S	032 39	295 09
2	07 04 66	19:58:04	44.25	7.42	5	44.12	7.39	6	4.4	BO	110 45E	135 48W	213 01	116 77
3	22 11 69	07:49:15	44.34	6.75	—	44.25	6.80	7	3.6	FR*	166 60W	110 46N	231 08	128 58
4	01 02 71	12:26:56	44.43	7.26	2	44.40	7.24	6	4.3	NI	150 55W	271 54N	120 56	211 01
5	06 06 71	21:59:11	44.77	6.73	2	44.63	6.75	3	4.2	NI	083 69N	160 60W	030 06	124 38
6	03 04 72	22:19:16	44.43	7.05	11	44.41	7.02	3	3.5	FR*	123 84S	038 50N	177 22	073 32
7	07 05 72	09:17:20	44.77	6.78	—	44.77	6.79	5	3.3	FR*	000 50W	130 53E	157 62	065 01
8	19 05 72	14:55:23	44.43	7.50	6	44.36	7.35	13	3.8	FR*	090 40N	158 73W	221 19	108 49
9	29 12 72	00:14:17	44.41	7.23	—	44.32	7.17	9	3.6	FR*	115 48E	162 52W	229 03	134 64
10	07 06 76	00:08:48	44.69	6.69	—	44.66	6.68	3	3.3	FR*	018 90	108 90W	063 00	333 00
11	09 10 76	00:35:10	44.65	6.85	1	44.57	6.91	8	3.6	FR*	177 70E	110 43W	310 49	060 16
12	27 12 76	15:39:30	44.81	6.83	8	44.79	6.88	3	3.4	FR*	004 48W	131 56E	066 05	164 60
13	06 02 77	16:01:31	44.52	7.34	10	44.49	7.34	5	4.0	FR*	120 48S	101 44E	201 02	098 80
14	24 06 77	05:51:49	44.52	7.32	9	44.46	7.38	11	3.6	FR*	138 46S	105 49N	031 02	126 73
15	03 03 77	12:13:25	44.69	6.69	7	44.66	6.64	7	4.0	FR*	156 47W	172 44E	174 82	074 01
16	09 08 77	15:31:24	44.59	6.89	0	44.51	6.92	4	3.6	FR*	164 74E	061 52N	210 39	108 14
17	23 09 77	22:34:11	44.37	7.38	8	44.29	7.39	8	3.6	FR*	134 70W	124 20E	221 25	050 65
18	24 09 77	04:08	44.52	6.87	2	44.44	6.92	3	2.5	FR*	000 22E	140 73W	030 60	241 27
19	03 10 77	01:32	44.52	6.87	4	44.54	7.08	3	3.0	FR**	170 26E	155 65W	052 70	250 20
20	03 10 77	01:49	44.52	6.86	3	44.46	6.86	4	2.8	FR**	174 30E	153 62W	040 71	251 16
21	30 09 78	01:30	44.51	6.85	8	—	—	—	—	FR**	166 70E	015 23W	239 63	084 24
22	30 09 78	09:13	44.51	6.85	6	—	—	—	—	FR**	000 74E	014 16E	264 61	093 29
23	30 09 78	09:41	44.51	6.86	8	—	—	—	—	FR**	167 70E	111 33W	292 57	057 21
24	01 10 78	20:11	44.50	6.84	8	44.19	7.43	4	1.8	FR**	144 82N	055 83S	189 01	280 11
25	03 10 78	12:38	44.48	6.89	9	—	—	—	—	FR**	024 56E	166 41W	346 69	097 08
26	06 10 78	00:45	44.47	6.89	11	44.40	7.31	15	2.0	FR**	032 60E	131 75W	355 33	259 10
27	04 12 79	08:47:39	44.40	7.30	4	44.29	7.39	15	3.5	FR*	112 64E	165 39W	043 14	158 59
28	10 10 80	21:42:50	44.48	7.06	8	44.37	7.15	6	3.3	FR*	117 49S	133 42N	215 03	328 81

Table 2 (*Continued*)

No.	Date	Times (h:min:s)	Lat. (N) (old)	Lon. (E) (old)	z (km) (old)	Lat. (N) (new)	Lon. (E) (new)	z (km) (new)	M	Meca. ref.	Pl. 1 (Az. Dip)	Pl. 2 (Az. Dip)	P axes (Az. Dip)	T axes (Az. Dip)
29	04 01 81	04:09:20	44.26	7.31	5	44.21	7.48	5	3.5	BE	050 84E	145 50W	104 22	360 32
30	03 06 82	11:38:12	44.30	7.43	4	44.33	7.39	5	3.7	NI	041 48W	131 90	184 28	078 28
31	22 12 83	18:12:21	44.32	6.75	3	44.27	6.73	6	3.5	BE	176 57E	100 70W	226 08	322 39
32	12 01 84	08:24:46	44.66	7.35	10	44.68	7.35	8	3.6	BE	005 20E	108 85W	215 37	358 46
33	21 02 85	18:00:34	44.37	7.42	14	44.30	7.51	4	3.2	BE	157 65W	105 37E	227 15	109 60
34	17 01 86	18:48:03	44.38	7.33	10	44.35	7.34	6	3.3	BE	030 33W	165 65E	219 63	092 17
35	11 03 86	07:46:38	44.40	7.32	5	44.32	7.39	10	3.6	BE	067 79W	161 70E	203 22	295 06
36	17 07 86	07:35:34	44.53	7.26	1	44.51	7.21	3	3.2	BE	045 45W	165 63E	206 55	101 11
37	09 05 87	06:00:17	44.23	6.77	2	44.16	6.86	6	3.4	BE	050 47E	160 70W	025 47	280 14
38	28 05 87	23:00:53	44.63	7.11	2	44.56	7.05	9	3.4	BE	055 70W	135 64W	004 04	096 33
39	15 06 87	21:27:18	44.41	7.31	10	44.30	7.42	8	3.3	BE	042 35W	095 67W	043 59	165 18
40	22 01 89	11:58:34	44.54	6.81	11	44.52	6.86	4	3.4	GU	164 66W	031 33E	217 61	091 18
41	25 01 89	03:16:58	44.53	6.80	9	44.53	6.86	3	3.4	GU	166 70W	036 30E	224 58	093 22
42	23 06 90	10:30:00	44.30	7.21	4	44.31	7.22	10	2.3	DE	145 71N	088 32S	269 56	035 22

(FR*): FRÉCHET, 1978, and MÉNARD and FRÉCHET, 1988; (FR**): FRÉCHET and PAVONI, 1979; (BO): BOSSOLASCO *et al.*, 1972; (BE): BÉTHOUX *et al.*, 1988; (NI): NICOLAS *et al.*, 1990; (GU): GUYOTON *et al.*, 1990; (DE): DEVERCHÈRE *et al.*, 1991.

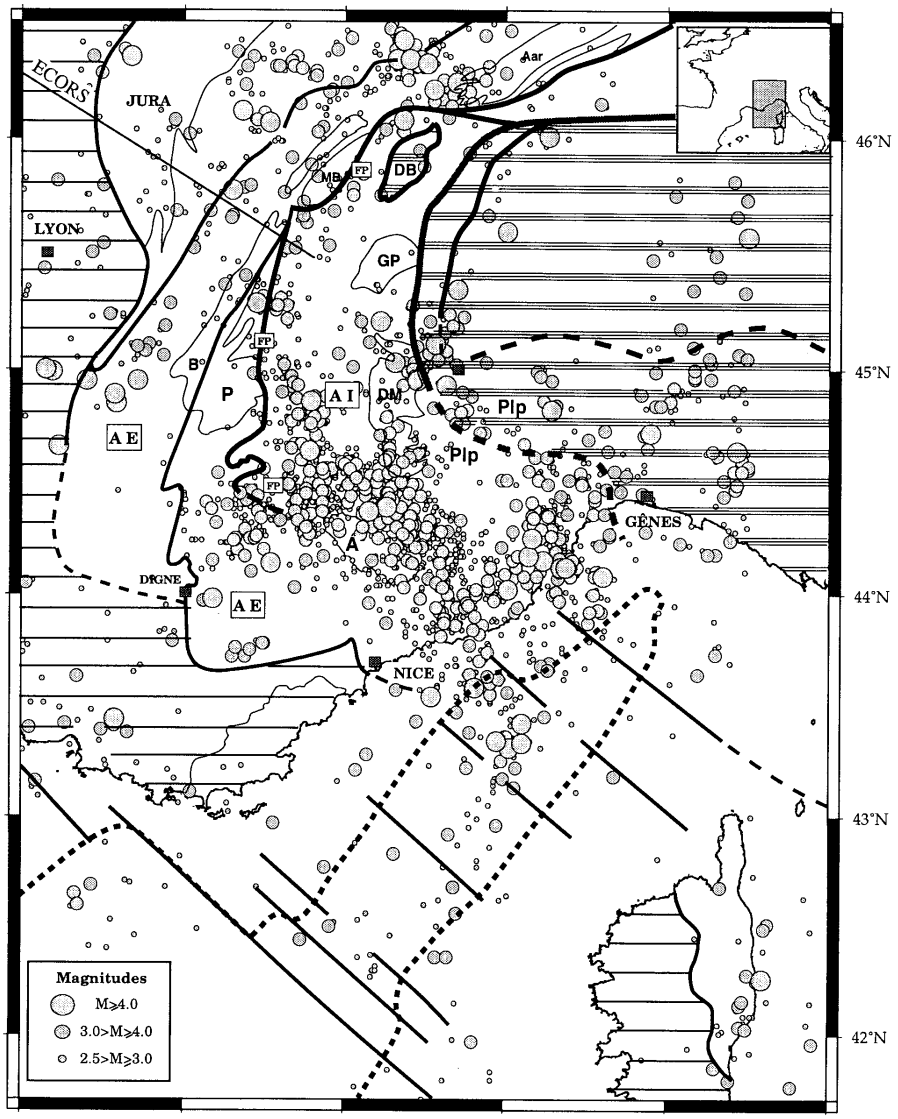

Figure 2
The seismicity map, superimposed on the tectonic map: AI: Internal Alps, AE: External Alps, FP: Penninic front, B: Briançonnais arc, Plp: Piemontais arc, A: Argentera, DM: Dora Maira, P: Pelvoux, B: Belledonne, MB: Mont Blanc, DB: Dent Blanche. The location of the ECORS-CROP seismic profile is displayed.

—First: the classical check of the validity of a location routine is the comparison of the calculated location of shots or quarry blasts with the true location.

—Second: obtaining a coherent epicentral distribution rather than a diffuse one is a visual argument overall if the map of earthquake epicenters outlines the superficial trace of the major fault structures (taking into account the bias linked to the slope of the faults at depth).

—Third: the superimposition of geological cross section (deduced from seismic profiles) with hypocenter distribution may also be an argument of analysis we will discuss further.

In a first step we have verified the mislocation of artificial events. The rockbursts in the mines of Gardanne, near Marseille, are a good opportunity to test the improvement of the locations versus the year of recording. Figure 3 displays the evolution of mislocation of these events (taking into account the accurate location of the contemporaneous face). This result can be an indicator of the degree of reliability of earthquake locations according to the year of occurrence. Note the break in the values of the shift between computed and true location, for 1983.

We also check recent quarry shots located in other regions, most of them are located with a depth between 0 and 2 km and in surface mislocated by less than 2.5 km. The second criterion of evaluation we use to evaluate the accuracy of the new

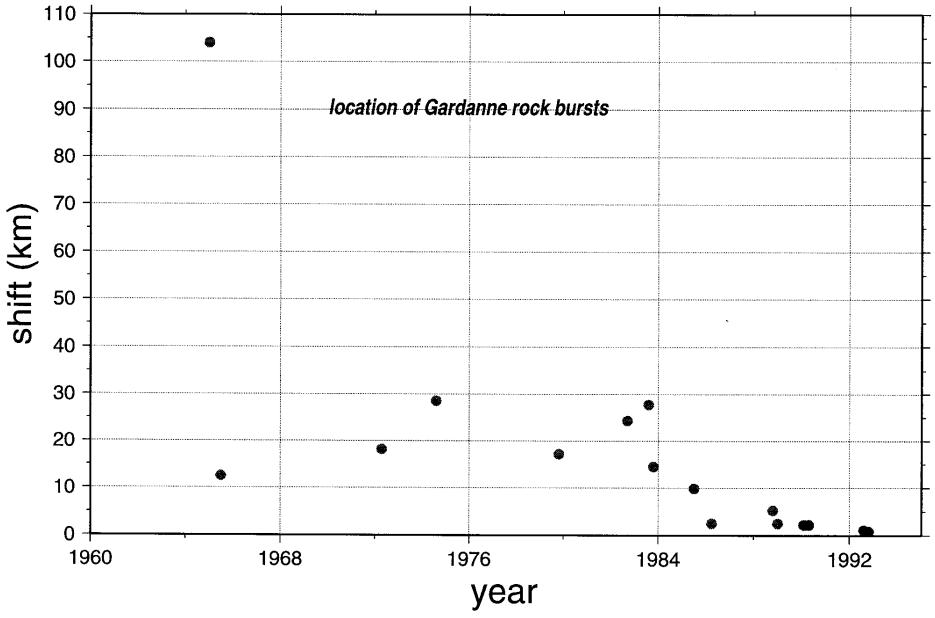

Figure 3
Evolution versus the year of recording, of the accuracy of the location of rockbursts from the coal mine of Gardanne. The shift between computed and true location is given in km.

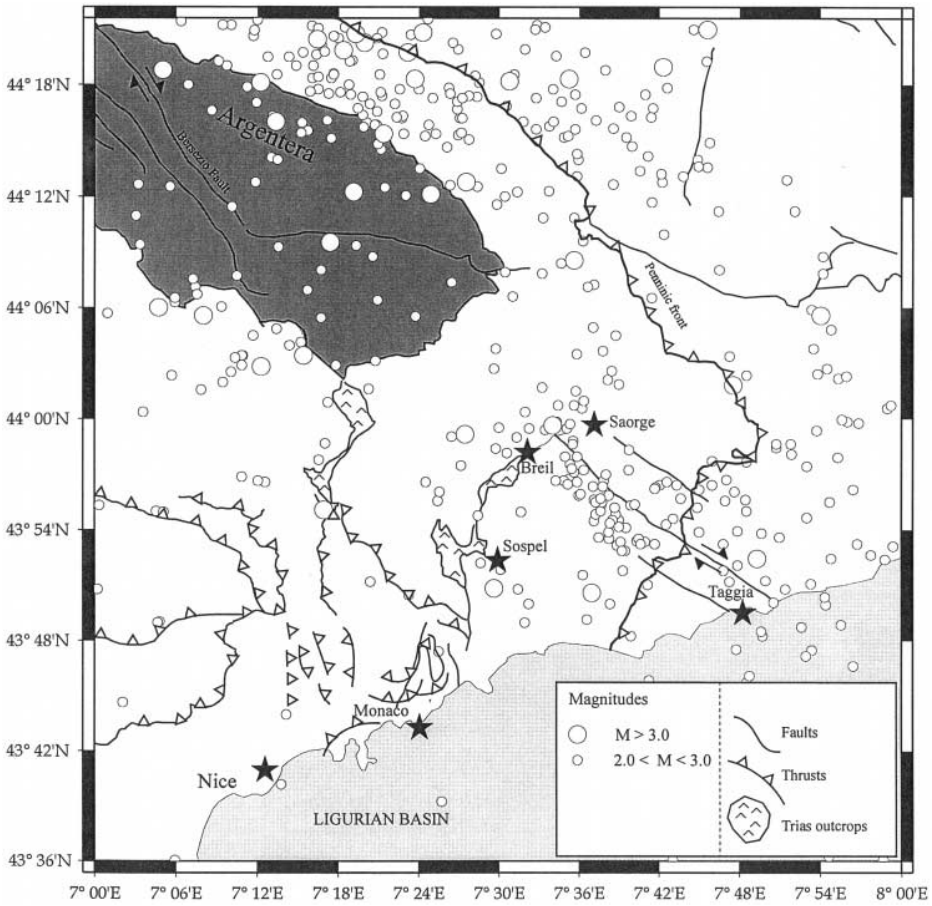

Figure 4
Seismicity of the southwestern Alps superimposed on a tectonic map. Villages are denoted by stars.

locations is a comparison of epicenter distribution against the known tectonic structures.

Figure 4 displays an example of such a comparison obtained for the southwestern Alps during the 1983–1993 period: a good agreement is found between the tectonic structures observed in the field and the epicenter distribution. Particularly, we can observe the seismicity along the southern prolongation of the Penninic front. An alignment of the epicenters corresponds to the right-lateral strike-slip fault of Saorge-Taggia and parallel faults, trending N130; a seismic crisis occurred there in 1983–1984 (HOANG-TRONG *et al.*, 1987). The conjugate direction N30 is recognized in the field by the fault Monaco-Sospel-Breil; although this fault is of

low seismic activity, the virgation known by geological observations appears in the distribution of epicenters. One interesting observation is the concentration of seismicity lined in exactly this direction N30 but in the northern prolongation of the Monaco-Sospel-Breil fault, which leads to postulate the continuation of this fault at depth.

If the entire catalogue is used, the coherency between accidents and epicenters is partly lost; before 1983, as already demonstrated by the location of rockbursts, a minimum dispersion of 10 km is estimated. This change coincides with the installation of several Italian stations of DISTER network (FIN, RSP) and of the station SBF (LDG/CEA), in the area under consideration. New improvement corresponds to the installation of ReNaSS network in 1986. Thereafter we tested the value of depth obtained by correlation with the ECORS-CROP profile interpretation (TRUFFERT *et al.*, 1990): the events, which occurred in a band of 20 km width centered on the profile (Fig. 2), are located around the location of the thrusts, as determined by wide angle reflection data (see Fig. 5) and more particularly on the eastern side of Belledonne massif. Considering the uncertainties of the position of the reflectors obtained by the seismic profile interpretation, and the uncertainties of the focal depths, we can conclude that the distribution of the foci in two groups of events (one is about 5 km deep, the other is about 20 km deep) does not correspond to errors of location (about 5 km in depth), and is linked to the structural characteristics of the region.

On Figure 6, we have superimposed the seismicity onto the map of Moho isobaths (after GRELLET *et al.*, 1993). We can observe that the distribution of the earthquakes follows the lines of the isobaths, without the events occurring systematically at the base of the crust. This fact only means that the seismogenic depth increased as the Moho depth. This behaviour may be linked to the presence of thrusts as we have mentioned. The earthquakes are numerous along the Penninic

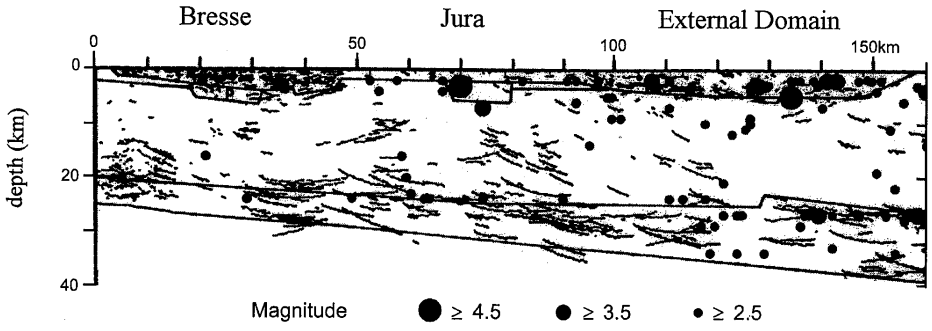

Figure 5
Foci of the events along the ECORS-CROP profile. The location of this profile is denoted on Figure 2, the interpretative section is after TRUFFERT *et al.*, 1990.

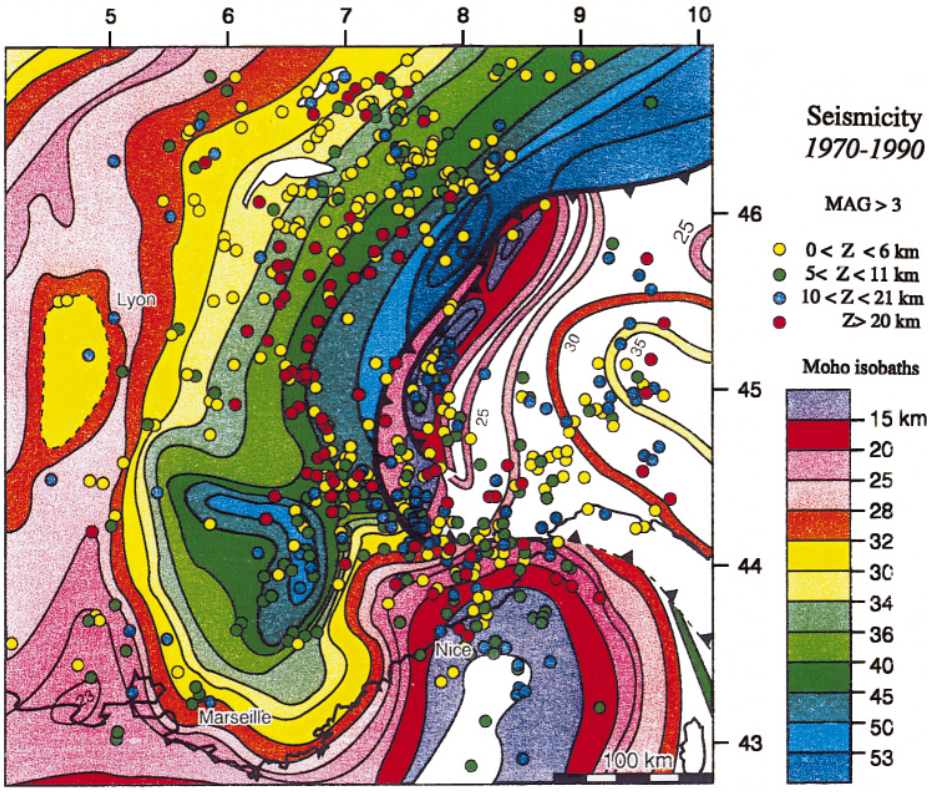

Figure 6
Seismicity versus the depth of the events superimposed on the map of the Moho isobaths after GRELLET *et al.* (1993).

front: the deepest events correspond to the eastern border of the external domain as observed in Figures 5 and 2; these deep foci have been observed in regional studies (DEICHMANN, 1987; CATTANEO *et al.*, 1987; GUYOTON, 1991); our more general map confirms these spatially limited observations.

From analysis of locations obtained for artificial events, we expect an accuracy of about 1 km in epicentral coordinates for the recent events (the period 1987–1993) and 5 km in depth. For the older events, located with only some arrival times most often incoherent among them, the location is much less constrained. We estimate that the errors reach several tens of kilometers, as demonstrated by the examples of the locations of rockbursts (Fig. 3) and of the aftershocks of the Vercors event of April 25, 1962 ($M = 5.3$): they comprise a swarm of around 50 km in length. Nevertheless, we kept these events in order to carry out the most complete study for this very short period of instrumental seismicity, on the

recurrence periods usually postulated for western Europe. The advantage of this catalogue lies in its homogeneity with respect to the location technique used, and the local magnitude determination, as we will show in the following sections.

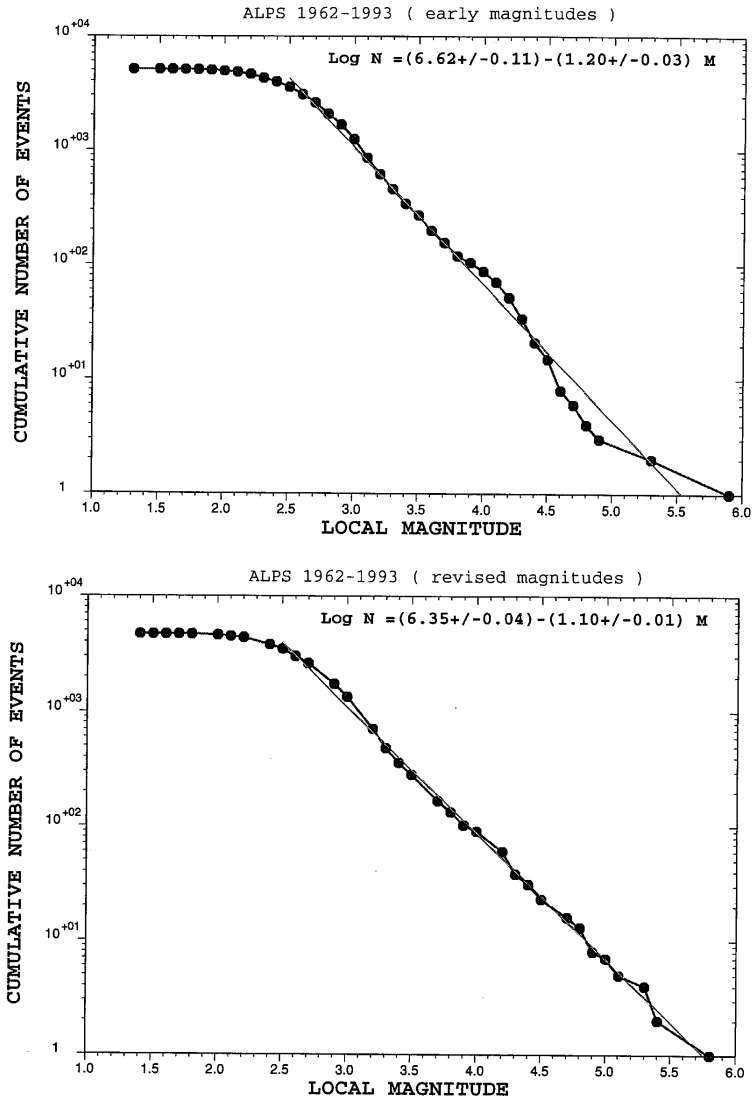

Figure 7
A—Curve of the frequency-magnitude distribution computed with previous magnitudes. B—Curve of the frequency-magnitude distribution computed with the revised magnitudes.

Revision of the Magnitudes

The discrepancies between the evaluation of the local magnitude, M_l, from one network to another is well known. However, even for a single network, it is also difficult to obtain a homogeneous scale of magnitude available for small as well as for major shocks. These difficulties are linked to the influence of the source and site effects on the amplitude recorded in a given station, overall if this station is too close to the epicenter.

The LDG network is a homogeneous network with the same sensor and recorder at all the stations. Some of these stations have been operative on the entire period investigated by the Bulletin (1962–1993). We have taken these advantages to build a scale of local magnitude as homogeneous as possible in space and in time. The first aim was to obtain a good consistency between local magnitudes M_l defined from the amplitude of S waves recorded by the LDG network and the M_b magnitudes depicted by the ISC Bulletins. For each station corrections have been adjusted for different ranges of epicenter distance and azimuth.

Before 1980 the duration magnitude, M_d, prevailed largely when only analog records were available, with a substantial part of them being saturated, due to the low dynamic range of the recorders (72 dB). Consequently, a statistical relation was sought between the M_l magnitudes and the M_d magnitudes, evaluated from the duration of the signal. The duration magnitude being evaluated by a formula such as $M_d = a + b^*$ log (duration time), the relation $M_l = a_i + b_i^*$ log (duration time) + $c_{i,j}$ has been adjusted to data by a least-squares method; a_i and b_i are coefficients corresponding to a geographic region i; $c_{i,j}$ is the correction for the station j where the epicenter is in the region i. In these kinds of computations the values of the coefficient are dependent on the network used. Only the stations installed since the sixties are therefore involved in the computations, in order to apply this evaluation to the most dated events.

The main result is a shift towards higher values of the revised M_d determinations as compared with the early evaluations, for magnitudes higher than 4. Some significant examples are:

—the 14/03/64 event located at 46.87°N 8.32°E, the previous magnitude was evaluated at 4.6 and the revised value reached 5.7.

—the 26/02/69 event (48.30°N, 9.05°E) is shifted from $M_d = 4.6$ to $M_d = 5.1$.

—the 24/03/67 event (46.4°N, 7.3°E) is shifted from $M_d = 4.3$ to 4.9.

To test the quality of this re-evaluation of the magnitudes (with $M_l = M_d$), we have reported the logarithm of the number of events versus the magnitude (M_l). The new magnitudes provide a better fit of the data to the Gutenberg-Richter law (Fig. 7); the slope of the curve (the coefficient b of the Gutenberg-Richter law) is 1.1, and the average detection threshold obtained for this instrumental period is the magnitude 2.4. The statistical uncertainty of magnitudes, determined by the LDG network, is generally ± 0.1. The seismicity of the period 1962–1993 is moderate,

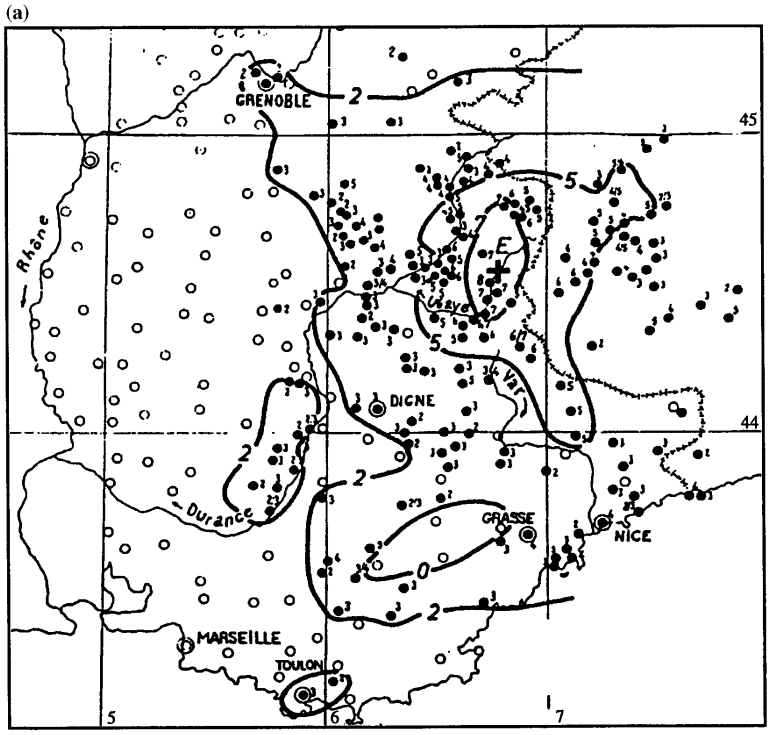

Fig. 8a

with 90% of magnitudes ranging from 2.5 to 3.5. Only eight events with magnitude higher than 5 occurred in this period.

The 1995–1962 Period

The year 1962 corresponds to the launching of the LDG network and the installation in France of twelve new stations, whereas before this date only three short-range stations (distance less than 300 km from the epicentral zone) were available west of the Alps. In order to recreate the past we have used the BCIS[3] Bulletin for the period 1955–1962 to test the possibility of improving the location of the highest energy events during this period; that is to say: the event of 30/03/1958, which occurred in Savoie region (near Annecy), the event of 05/04/1959 of Saint Paul d'Ubaye, the events of 04/01/1956 and 23/03/1960, both which occurred in the Valais region, near Sion, and the events of 12/05/1955 and 20/06/1955, located in the Cuneo area.

[3] BCIS: Bureau Central International de Séismologie, Strasbourg, France.

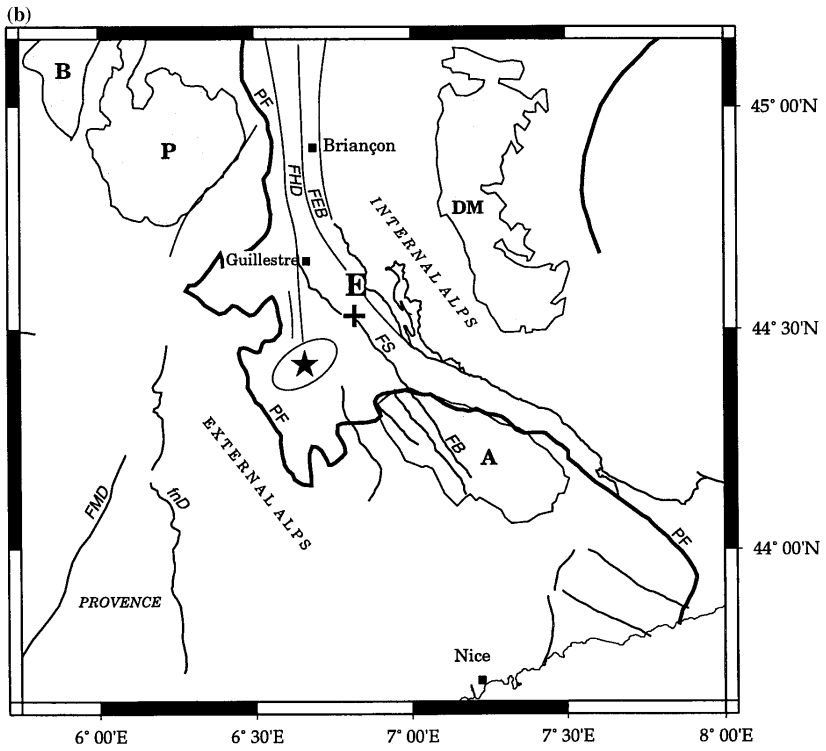

Figure 8
(a)—Isoseist map for the 1959 Ubaye event, after ROTHÉ (1967). (b)—Tectonic map of Ubaye region. The macroseismic (+) and instrumental (*) epicenters, and the confidence ellipse from the instrumental location are superimposed. FHD: Haute Durnance fault; FS: Sérenne fault; FB: Bersezio fault.

With the standard earthquake location algorithm in use at LDG/CEA, we obtained the results reported in Table 3. The relatively large number of time readings for these seven earthquakes balances the lack of precision of the clocks used in the seismological observatories in the period 1950–1960. Therefore the rms are rather small (Table 3).

What is the reliability of these locations? Even if the instrumental and macroseismic location cannot be directly compared, due to the possible occurrence of site effects, the contours of the isoseist lines can provide information on the location of an earthquake; if they are concentric and rather regular, we can assume the epicenter is likely to be located in the area of highest intensity.

The epicenters of Table 3 are about 10–20 km away from the macroseismic locations, provided by ROTHÉ (1967) and PAVONI (1977). We obtain confidence

Table 3

Location of 7 strongest events which occurred in the years 1955 to 1960. The statistical parameters of the computation are displayed. These locations are compared with the macroseismic epicenters

Date	Time	Lat. (°N) inst.	Lon. (°E) inst.	Depth (km)	Mag.	Number stations	rms (s)	Lat. (°N) macro	Lon. (°E) macro	I_0 (MSK)
120555	14h16	44.45	7.09	4	4.7	12	2.7	44.53	7.30	VII
200655	4h47	44.51	7.35	8	4.8	12	2.1	44.53	7.30	VII
040156	18h29	46.30	7.18	23	3.6	12	2.8	46.40	7.25	IV
040156	22h22	46.34	7.31	24		9	5.1	46.40	7.25	
300358	16h10	45.79	5.74	10	4.3	18	1.8	45.77	5.80	VI
050459	10h47	44.42	6.66	8	5.3	26	1.1	44.53	6.82	VIII
230360	23h08	46.41	8.16	2	5.2	25	1.3	46.35	8.08	VIII

ellipses in the same range of size. The 1959 shock which occurred in Haute-Ubaye is an example of such a comparison: Figure 8a shows the isoseist lines and macroseismic epicenter after ROTHÉ (1967); this one has been reported on the structural map (Fig. 8b) and compared with our instrumental location. The macroseismic epicenter could correspond to the Sérenne fault, the instrumental one to the southern prolongation of the Haute Durance fault. In any event, they both confirm the activity of the Haute Durance fault system (TRICART *et al.*, 1996), although the location on the Haute Durance fault is in better agreement with one nodal plane of the focal mechanism (Table 2).

The microseismicity is generally recorded with few stations and their number (taking into account the errors on arrival times) is not sufficient to obtain realistic locations (rms and axes of confidence ellipses corresponding to very high values). Except for the strongest events, it is not possible to improve the location of Alpine earthquakes before the early sixties.

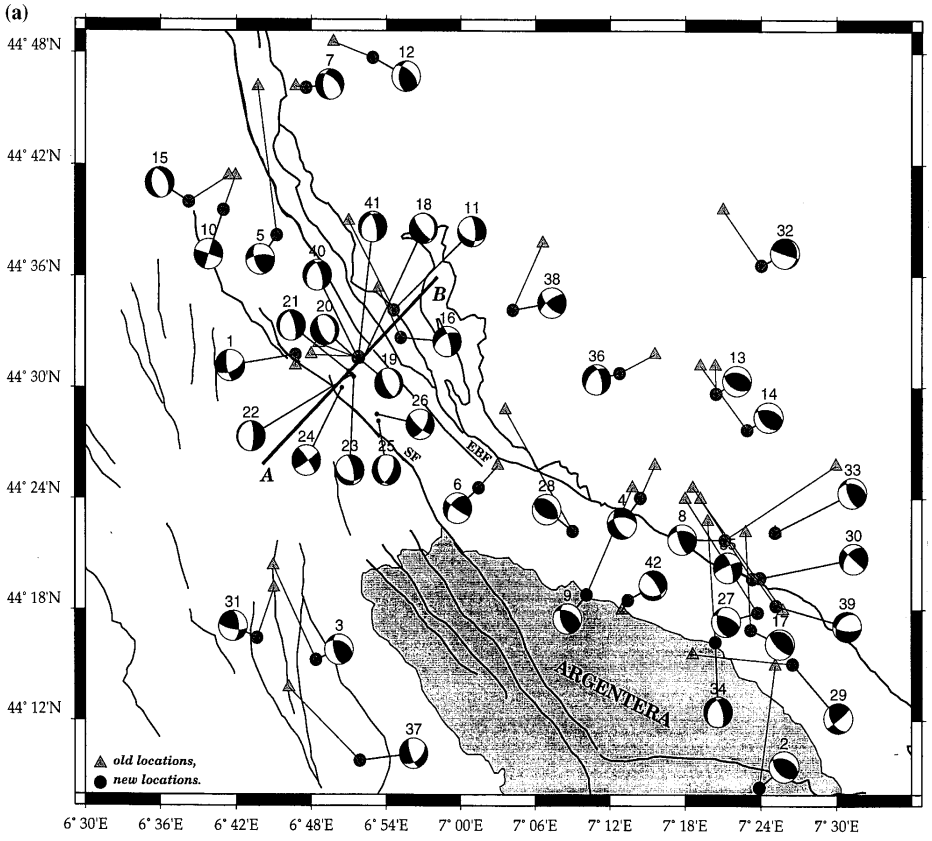

Fig. 9a

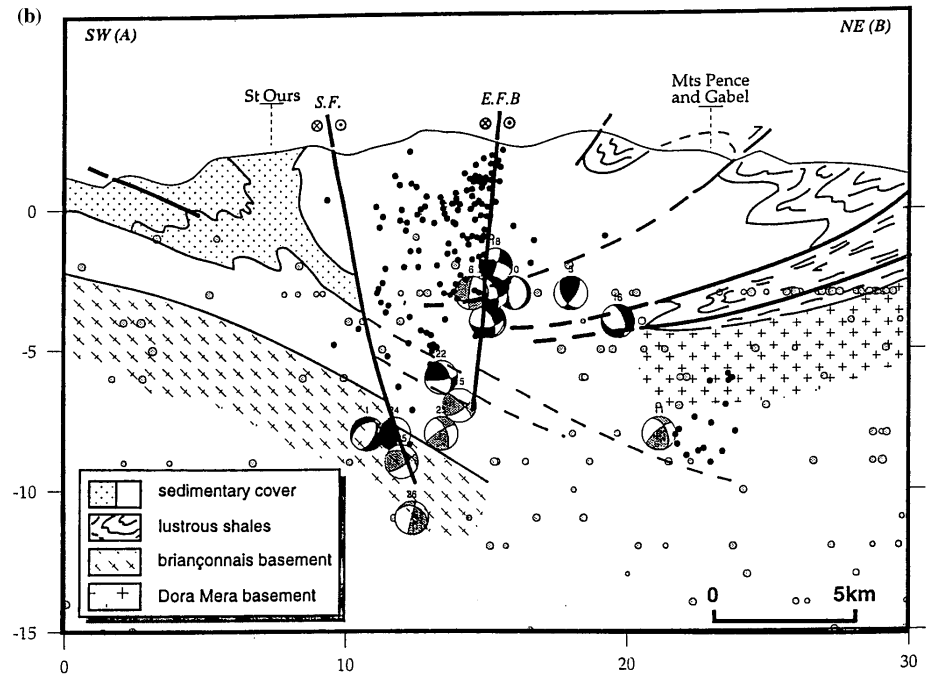

Figure 9
(a)—Focal solutions obtained for the Haute-Ubaye region and the line A-B, corresponding to the geological section after MÉNARD (1988). SF: Sérenne fault, EFB East Briançonnais fault. (b): The geological section, after MÉNARD (1988). The seismic crises studied by FRÉCHET and PAVONI (1979) are reported in black dots; the events of this catalogue in grey dots. The vertical projection of focal mechanisms from events located in a strip 30-km wide is superimposed.

Tectonic Implications for the Haute-Ubaye Region

To discuss the seismicity of the Haute-Ubaye region, an area located between the Pelvoux and Argentera massifs, we first started from the results obtained thanks to two seismological surveys conducted in 1977 and 1978 by FRÉCHET and PAVONI (1979). These authors located a swarm of 250 microseismic events (M_l ranging from 0.5 to 3.6), with an accuracy of ± 1 km or better, thanks to a dense network installed close to the seismogenic area. MÉNARD (1988) reinterpreted their results in the light of his own work on the geology and tectonics of the Western Alps. We use his geological vertical profile, obviously interpretative at depth. The location of his section (AB) is reported on Figure 9a, 30 km long with an azimuth of 45N, roughly perpendicular to the mean direction of the geologic structures. Ménard reported on this section the seismic swarm located by Fréchet and Pavoni (the black dots on Figure 9b). We superimposed the seismicity of our own catalogue on his

profile, projected from a strip 15-km wide on each side of the line AB (the grey dots on Figure 9b).

The permanent network recorded only the strongest magnitudes of the crises of 1977 and 1978, for which FRÉCHET and PAVONI (1979) computed focal mechanisms. Their locations and ours are compared in Table 2. Because our catalogue is considerably less limited in time (4 months in 77–78 compared to 32 years from 1962 to 1993) and not restricted to the study of a precise area, the distribution of foci spreads outside the zone confined between the dextral strike-slip Sérenne fault and the bundle of Est-Briançonnais strike-slip faults, which corresponds to the front of the Briançonnais internal units (Figs. 9a and b). The depths computed are rather shallow, reaching 15 km, in good agreement with previous studies. The seismicity is not randomly distributed. The region East of the Sérenne fault seems more active; west of this fault only some events are located above 5 km, guided by the thrust. The distribution of seismicity leads to the postulate that the Sérenne fault deepens to at least 10 km, taking into account the imprecision of earthquake depth (about 5 km).

Focal solutions computed by several authors (BOSSOLASCO *et al.*, 1972; FRÉCHET, 1978; FRÉCHET and PAVONI, 1979; BÉTHOUX *et al.*, 1988; MÉNARD and FRÉCHET, 1988; NICOLAS *et al.*, 1990; DEVERCHÈRE *et al.*, 1991) are reported on Figure 9a. FRÉCHET and PAVONI (1980), THOUVENOT *et al.* (1991), have pointed out the complexity of this area which is mainly submitted to an extensive component, but where all kinds of focal solutions are observed. For the events under study, the shift between previous locations and ours is represented by a line linking the two epicenters (Fig. 9a). We have reviewed that this shift is not important enough (see Table 2) to bring appreciable change in the focal solutions (not strongly constrained for the oldest events). We have kept the locations reported by Fréchet and Pavoni for the reasons previously explained (solutions 18 to 26, see Table 2). For the other events (not belonging to the crisis of 1977–1978), the revised locations allows us to refine the deformation along the Penninic front and along a family of parallel faults (Fig. 9a). Some previous determinations did not provide an estimation of the focal depth. One of the aims of the revised catalogue was to improve the accuracy of the depth using a crustal model which best pictures the area under study.

We have projected on the vertical cross section, the focal solutions obtained for the events located along the profile AB; this kind of projection requires a transformation of the representation of the nodal planes, whereas the usual representation is the projection of a lower hemisphere half space onto the horizontal plane. Figure 10 displays a theoretical example of such a transformation; which makes easier the comparison between the vertical crosscut of the faults and the direction of nodal planes. The vertical projection on the geological section (Fig. 9b) shows that these events are mainly located in the strike-slip corridor formed by the two faults referred above, which seem to focus the 'strongest' events of the region (M_l ranging

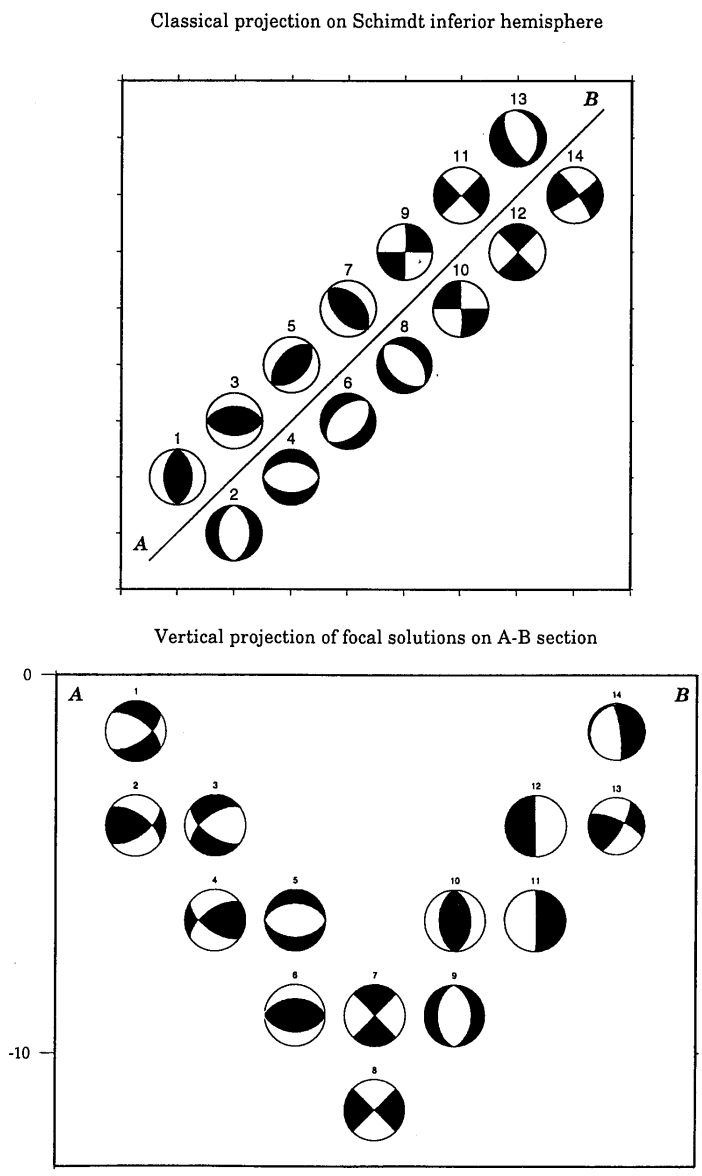

Figure 10
Theoretical examples of the vertical projection of focal solutions.

from 3.0 up to 4.3). The event 24, a pure right lateral strike-slip mechanism allows the geometry of the Sérenne fault to constrain at depth; we can conclude that this feature remains quite vertical up to about 10 km deep, whereas other neighbour

focal solutions have an extensive component linked to the presence of normal faults associated, recognized in the area in study but not reported in this profile. Recent microtectonic data confirm that these faults, parallel to the chain, demonstrate a regional extension, and that the thrust surface had been reactivated in extension at depth (TRICART *et al.*, 1996). The focal solutions 6 and 18, which are transtensive mechanisms, are coherent with the prolongation at depth of the second fault (one focal plane corresponds to the orientation of the fault).

Furthermore, we have represented in dark the mechanisms with the horizontal projection of *P*-axis trending NE-SW, in grey the horizontal projection of *P*-axis trending NW-SE. We obtain coherent representation of the focal solutions with two clusters which are rather well differentiated (Fig. 9b). We postulate that this division between two groups of events corresponds to the influence of the thrusts and overthrusts known in the region, according to the agreement between the depths of the limit between the two groups and the depth of these thrusts after the geological section.

What is the tectonic meaning of this change of direction of *P* axis? Note that these events generally correspond to low magnitudes. It is demonstrated that there can be local reorientation of stress direction near an accident (RAWNSLEY *et al.*, 1987). The observed reorientation of stress could only be due to the geometry of the thrusts.

Conclusion

Several examples we have worked out illustrate the utility of building earthquake catalogues, even if it is not possible to reach accurate locations for old events. The homogeneity in the construction of our catalogue warrants the reliability of results obtained at the scale of the entire Western Alps and southeast of France. An initial example is the computation of the parameters of the Gutenberg-Richter law, which needs homogeneous estimation of the magnitude in space as well as in time. The evaluation of depth using a unique algorithm allows us to globally look at the distribution of deep foci along the limit between external and internal zones, and is in good agreement with previous regional studies in regions such as the Mollasse Bassin (DEICHMANN, 1987).

Our catalogue allows us to perform regional seismotectonic analysis. As an example, we have demonstrated the rather good coherence between the distribution of epicenters and the location of the geological shallow accidents in the Southern Alps, where some hidden continuation of these structures can be postulated. Along the Ecors profile, as well as in the Haute-Ubaye region, we have pointed out the key role of Alpine thrusts and overthrusts in the distribution of foci.

Finally, the construction of such a catalogue is the preliminary step before carrying out a spatio-temporal seismological analysis in order to refine seismic hazard analysis.

Acknowledgements

We are grateful to the staff of the DISTER who provided their data base for the 1987–1991 period. We thank the two anonymous reviewers for their helpful critical comments. We thank B. Feignier, B. Massinon, J.L. Plantet and J.P. Santoire for their assistance. Contribution No. 179 of U.M.R. Geosciences Azur.

REFERENCES

AUGLIERA, P., CATTANEO, M., and EVA, C. (1995), *Seismic Multiplets Analysis and its Implication in Seismotectonics*, Tectonophys. *248* (3–4), 219–234.

BECK, C., MANALT, F., CHAPRON, E., VAN RENSBERGEN, P., and DE BATIST, M. (1996), *Late Quaternary Seismicity and Post-glacial 'Rebound'; Data from Sedimentary Recording in Lake Annecy, Northwestern Alps*, J. Geodyn. *22* (1/2), 155–171.

BÉTHOUX, N., CATTANEO, M., DELPECH, P. Y., EVA, C., and RÉHAULT, J. P. (1988), *Mécanismes au foyer de séismes en mer ligure et au sud des Alpes occidentales: résultats et interprétations*, C. R. Acad. Sci. Paris *307*, 71–77.

BLUNDELL, D., FREEMAN, R., and MUELLER, S., *A Continent Revealed: The European Geotraverse* (Cambridge University Press 1992) 275 pp.

BOSSOLASCO, M., CICCONI, G., EVA, C., and PASQUALE, V. (1972), *La rete sismica de l'Istituto Geofisico di Genova e primi risultati sulla sismo-tettonica delle Alpi Marittime ed Occidentali, e del Mar Ligure*, Riv. Ital. Geofis. *XXI*, 229–247.

CAPONI, G., EVA, C., and MERLANTI, F. (1980), *Some Considerations on Seismotectonics of the Western Alps*, Boll. Geof. Teor. Appl. *22* (87), 223–240.

CATTANEO, M., EVA, C., MERLANTI, F., and PASTA, M. (1987), *Analisi della sismicita della Liguria Occidentale dal 1982 al 1986*, Atti del VI conv. G.N.G.T.S. Roma, 14–16 December, 295–305.

CLOSS, H., and LABROUSTE, Y. (1963), *Recherches sismologiques dans les Alpes occidentales au moyen des grandes explosions en 1956, 1958 et 1960*, Mém. collec. du groupe d'étude des explosions alpines, CNRS ed., p. 241.

DEICHMANN, N. (1987), *Focal Depths of Earthquakes in Northern Switzerland*, Ann. Geophys. Paris *5B* (4), 395–402.

DEVERCHÈRE, J., BÉTHOUX, N., HELLO, Y., LOUAT, R., and EVA, C. (1991), *Déploiement d'un réseau de sismographes sous-marins et terrestres en domaine ligure (Méditerranée): campagne SISBALIG 1*, C.R. Acad. Sci. Paris *313*, 1023–1030.

EVA, C., AUGLIERA, P., CATTANEO, M., and GIGLIA, G., *Some considerations on seismotectonics of northwestern Italy*. In *The European Geotraverse: Integrative Studies* (eds. Freeman, R., Giese, P., and Mueller, St.) (European Science Foundation, Strasbourg 1990) pp. 289–296.

FRÉCHET, J. (1978), *Sismicité du Sud-Est de la France, une nouvelle méthode de zonage sismique*, Thèse de 3° Cycle, Univ. Grenoble, 159 pp.

FRÉCHET, J., and PAVONI, N. (1979), *Etude de la sismicité de la zone briançonnaise entre Pelvoux et Argentera (Alpes Occidentales) à l'aide d'un réseau de stations portables*, Eclogae Geol. Helv. *72/3*, 763–779.

GEIGER, L. (1910), *Herdbestimmung bei Erdbeben aus den Ankunftszeiten*, K. Gesell. Wiss. Gott. *4*, 331–349.

GRELLET, B., COMBES, P., GRANIER, T., and PHILIP, H. (1993), *Sismotectonique de la France métropolitaine dans son cadre géologique et géophysique*, Mém. Soc. Géol. de France *164* (2), 24 pl., 75 pp.

GUYOTON, F. (1991), *Sismicité et structure lithosphérique des Alpes occidentales*, Thèse de Doctorat, Univ. Grenoble, 290 pp.

GUYOTON, F., FRÉCHET, J., and THOUVENOT, F. (1990), *La crise sismique de janvier 1989 en Haute-Ubaye (Alpes-de-Haute-Provence, France): étude fine de la sismicité par le nouveau réseau SISMALP*, C.R. Acad. Sci. Paris *312*, 985–991.

HENDRICKX, S. (1981), *Prévision à court terme de séismes dans un contexte de prise de décision. Application à la région du Sud-Est de la France*, Thèse de Docteur-Ingenieur, Ecole Centrale des Arts et Manufactures, 203 pp.

HOANG-TRONG, P., HAESSLER, H., HOLL, J. M., and LEGROS, Y. (1987), *L'essaim sismique (Oct. 83–Jan. 84) de la moyenne vallée de la Roya (Alpes-Maritimes): activité récente d'un ancien systéme de failles conjuguées?* C.R. Acad. Sci. Paris *304*, 419–424.

KISSLING, E., SOLARINO, S., and CATTANEO, M. (1995), *Improved Seismic Velocity Reference Model from Local Earthquake Data in Northwestern Italy*, Terra Nova *7*, 528–524.

KLEIN, R. W. (1978), *Hypocenter Location Program HYPOINVERSE, I, Users Guide to Versions 1, 2, 3 and 4*, U.S. Geol. Surv. Open-file Rep., 78–694.

LAHR, J. C. (1980), *HYPOELLIPSE/MUTICS: A Computer Program for Determining Hypocenter, Magnitude, and First Motion Pattern*, U.S. Geol. Surv. Open-file Rep., 80–59.

LEE, W. H. K., and LAHR, J. C. (1975), *A Computer Program for Determining Hypocenter, Magnitude, and First Motion Pattern of Local Earthquakes*, U.S. Geol. Surv. Open-file Rep., 75–311.

LEVRET, A., BACKE, J. C., and CUSHING, M. (1994), *Atlas of Macroseismic Maps for French Earthquakes with their Principal Characteristics*, Natural Hazards *10*, 19–46.

MÉNARD, G. (1988), *Structure et cinématique d'une chaîne de collision: les Alpes occidentales et centrales*, Thèse de Doctorat d'Etat, Univ. Grenoble, 268 pp.

MÉNARD, G., and FRÉCHET, J. (1988), *Mécanismes au foyer de séismes des Alpes occidentales et modèle de déformation actuelle de la chaîne*. In *Structure et cinématique d'une chaîne de collision: les Alpes Occidentales et Centrales* (ed. Ménard) (Thèse de Doctorat d'Etat, Univ. Grenoble) p. 268.

NICOLAS, M., SANTOIRE, J. P., and DELPECH, P. Y. (1990), *Intraplate Seismicity: New Seismotectonic Data in Western Europe*, Tectonophysics *179*, 27–53.

PAVLIS, G., and BOOKER, F. (1983), *Progressive Multiple Event Location*, Bull. Seismol. Soc. Am. *73*, 1753–1777.

PAVONI, N. (1977), *Erdbeben im Gebiet der Schweiz*, Eclogae geol. Hel. *70* (2), 351–370.

PAVONI, N., and ROTH, P. (1990), *Seismicity and Seismotectonics of the Swiss Alps: Results of Microearthquake Investigations 1983–1988*, Mém. Soc. Géol. de France *156*, Mém. Soc. Géol. Suisse *1*, Mém. Soc. Geol. Italiana *1*, 203–216.

RAWNSLEY, K. D., RIVES, T., PETIT, J. P., HENCHER, S. R., and LUMSDUN, A. C. (1992), *Joint Development in Perturbed Stress Fields Near Faults*, J. Struct. Geol. *14* (8/9), 939–951.

ROTHÉ, J. P. (1942), *La séismicité des Alpes occidentales*, Bull. Soc. Géol. Fr. *5*, II, 295–320.

ROTHÉ, J. P. (1967), *La séismicité de la France de 1951 à 1960*, Annales de l'Institut de Physique du Globe de Strasbourg *VIII*, 19–84.

ROURE, F., HEITZMANN, P., and POLINO, R. (1990), *Deep Structure of the Alps*, Mém. Soc., Géol. France *156*, Mém. Soc. Géol. Suisse *1*, Mem. Soc. Geol. Italiana *1*, 345 pp.

THOUVENOT, F., FRÉCHET, J., VIALON, P., GUYOTON, F., and CATTANEO, M. (1991), *Les séismes de Cervières (Hautes Alpes) des 11 et 13 février 1991: un coullissage dextre entre zones piémontaise et briançonnaise*, C.R. Acad. Sci. Paris *312*, II, 1617–1623.

TRICART, P., BOUILLIN, J. P., DICK, P., MOUTIER, L., XING, C. (1996), *Le faisceau de failles de haute-Durance et le rejeu distensif du front briançonnais au SE du Pelvoux (Alpes occidentales)*, C.R. Acad. Sci. Paris *323*, II, 251–257.

TRUFFERT, C., BURG, J.-P., CAZES, M., BAYER, R., DAMOTTE, B., and REY, D. (1990), *Structures crustales sous le Jura et la Bresse: contraintes sismiques et gravimétriques le long des profils Ecors Bresse-Jura et Alpes II*, Mém. Soc. Géol. de France *156*, Mém. Soc. Géol. Suisse *1*, Mem. Soc. Geol. Italiana *1*, 157–164.

(Received November 27, 1996, accepted May 4, 1998)